



46th SME North American Manufacturing Research Conference, NAMRC 46, Texas, USA

# Structural Optimization of a Direct-Drive Wind Turbine Generator Inspired by Additive Manufacturing

Austin Hayes<sup>a\*</sup>, Latha Sethuraman<sup>b#</sup>, Katherine Dykes<sup>b</sup>, and Lee Jay Fingersh<sup>b</sup>

<sup>a</sup>*Rochester Institute of Technology, 1 Lomb Memorial Drive, Rochester, New York 14623, USA*

<sup>b</sup>*National Renewable Energy Laboratory, 15013 Denver West Parkway, Golden, CO 80401*

\*Corresponding author. Tel.: 1-330-840-1875

E-mail address: [ach6895@rit.edu](mailto:ach6895@rit.edu)

#E-mail address: [Latha.Sethuraman@nrel.gov](mailto:Latha.Sethuraman@nrel.gov)

## Abstract

This study explores the structural freedom and design opportunities of additive manufacturing for a 5-MW direct-drive generator for a wind turbine and compares it to more traditional spoke-arm designs using NREL's GeneratorSE. The work focuses on light-weighting the stator within the generator, complementing previous rotor work. The light-weighting approach uses complex geometries and lattice structures made possible by additive manufacturing to realize increased strength with reduced mass. By reducing the mass at the top of the tower, wind turbines face lower loading along with decreased cost and improved structural stability. Furthermore, an altered bedplate support location facilitates lighter stator designs by better load transfer. Design optimization suggests additive manufacturing has the potential to transform generator designs to realize light-weighting. Since these machines are large, simulation and modeling are essential first steps before future experimental validation.

© 2018 The Authors. Published by Elsevier B.V.

Peer-review under responsibility of the scientific committee of the 4th International Conference on System-Integrated Intelligence.

*Keywords:* additive manufacturing, light-weighting, direct drive generator, stator, wind turbine, simulation/modeling

## 1. Introduction

When designing wind turbines, reducing top-head mass is of importance because it enables the ability to build larger and taller wind turbines that can harness more powerful winds at greater heights. The

choice of a drivetrain is also critical, especially when the generator impacts several factors (including mass, efficiency, operation and maintenance, reliability, and overall cost of energy). Additionally, drivetrain choice is of great importance for offshore wind turbines, where there are significant trade-offs

between material usage, cost of components, weight of the overall system and reliability, which significantly impacts offshore wind project operational expenditures.

A classic configuration for land-based wind applications are multistage gearboxes that allow for the use of high speed, low-torque operation of generators that are smaller, lightweight, and inexpensive to build. Gearboxes have many mechanical load-bearing components that are prone to reliability issues. Since accessing offshore wind power plants is difficult, any gearbox failure in an offshore wind plant can lead to significant downtime for the turbine and lost energy production, as well as expensive maintenance operations due to logistical challenges of getting equipment and personnel to the site. Thus, many manufacturers of offshore wind turbines are developing products with direct-drive technologies for their drivetrains.

Direct coupling of the generator to the turbine leads to low-speed high-torque machines with high pole count and large stator diameters that pose remarkable design and manufacturing challenges [1]. Generators employing permanent magnets are designed in different electromagnetic flux topologies employing nonstandard design architectures. Most permanent magnet machines are radial flux machines (i.e., the magnetic field runs radially with respect to the direction of the rotor shaft). These machines can be produced with nearly the same manufacturing methodology as induction machines because the layout for both machine types are similar. However, this approach is not an optimal solution for all cases [2]. Because high magnetic forces constantly act between the rotor and stator, accurately fixing the position of the stator teeth and the windings in the stator is immensely challenging. The air gap between the stator and rotor must be kept uniform and small for proper torque transfer and designers are constantly seeking measures for controlling or minimizing eccentricity to prevent potentially fatal distortions.

For instance, pure torque design uses an elastic coupling to isolate the massive 8-meter diameter generator from nonrotational loads that cause eccentricity [3]. Other designs [4] employ substantial spoke-and-rim wheel structures that need to be built up by welding overly thick steel elements. As wind turbines become larger in diameter, constructing them as a single module (i.e., continuous one-body structure) is disadvantageous in terms of manufacture

and maintenance. Hence, manufacturers resort to segmented configurations to facilitate transport and assembly. Modular designs (i.e., bolted assemblies) that simplify manufacturing have been proposed. Such designs, however, are not commercialized for assembly because they have tolerance management, noise, and vibration issues that are highly complex and expensive to minimize [4]. Furthermore, the mass of a direct-drive generator within traditional designs has a power rating of 10-MW and ranges between 200-500 tons [5]. A 15-MW version would be prohibitively massive and infeasible to manufacture.

In the past, several researchers have considered optimizing direct-drive generator designs [6,7] that focus on structural mass reduction through topology optimization [8-10]. More recently, attempts have been made to investigate designs that can reduce generator manufacturing costs. For example, Semken [11] proposed slanted spoke structural wheel architectures that were constructed using layered sheet-steel elements to form the spokes and the rim of the wheel faces. Tassarolo et al. [1] proposed a highly modular design to segment the generator into independent units, which can be connected in parallel and used to feed separate power converters. In this instance, the generator design had intrinsic fault tolerance through simple part replacement repairs in case of a fault. In an application such as a wind turbine, direct-drive electric generators can be subjected to continual flexing and extreme temperatures that are potentially catastrophic. Eliminating deep structural welds can significantly reduce manufacturing cost and also avoid problems associated with fatigue cracking and failure of welded connections [11]. At the same time, as the demand for direct-drive generators grows, manufacturers seek to create new technological solutions, such as additive manufacturing (AM), that facilitate mass production at competitive costs.

In recent years, metal additive manufacturing is gaining prominence and emerging across a broad range of sectors, including automotive, medical and aerospace. A vast range of metallic materials, (including several steels, titanium, cobalt and aluminium alloys) are printable, and newer materials for soft-magnetic cores are recently introduced [12]. Inspired by recent advances in steel and iron core printing, this study explores the structural freedom and design opportunities for a 5-MW direct drive generator. We will specifically evaluate two stator

designs: the square lattice and U-beam spoked lattice design based on their structural performance under generator loading. The objective is to use these designs catered for additive manufacturing to reach an optimum solution with decreased stator deflection and decreased mass. Finite element analysis is used to determine stator deflections and evaluate design performance. The remnant flux density is iterated between a minimum and maximum and the increased deflections calculated for both designs. The rest of the paper is organized as follows. Section 1 provides a review of previous work on structural lightweighting of large direct-drive generators and identifies a feasible process for large-scale metal additive manufacturing. Sections 2 and 3 present the analysis approach and introduce the stator designs. The influence of bedplate support is discussed in section 4. The potential for lightweighting inspired by AM and structural optimization is presented in the conclusions.

### 1.1 Structural lightweighting of direct-drive generator and additive manufacturing

Conventional direct drive generator support structures for radial flux machines are made of spoked-wheel structures that support rims of iron/magnetic core laminations. Typical geometries are disks, structural profiled spokes/tension rods, ribs or support structures (Figure 1); their structural stiffness and interfaces are controlled by manufacturing tolerances [4]. Variations in stator structural design are due to trade-offs in weight and strength as well as variation in load transfer designs.

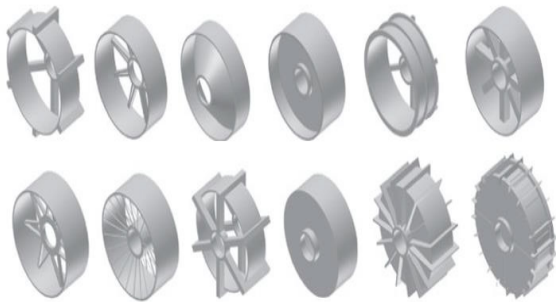


Figure 1: Conventional generator stator and rotor support structures [4]

Because conventional direct-drive generator support structures operate at low rotational speeds, their corresponding torques and diameters must be made large enough to generate the required power output. The air-gap separating the rotor and stator is typically 1/1000 of its diameter. Any eccentricity in the gap or inadvertent closing of the airgap is a major concern in permanent magnet direct drive (PMDD) generators. Eccentricity is further exacerbated by negative stiffness of magnets that have the potential to lower the air-gap distance in localized areas resulting in uneven loading and increased deformation. These effects cause the structural designs to be extremely rigid and excessively massive. Spokes must be increased dimensionally and in quantity, or the discs must be made stiffer by adding more steel. Spokes and disks can be manufactured as continuous cast iron or segmented steel weldment assemblies that yield stiffer structures per unit mass; however, they are expensive to build.

By changing the design or materials (e.g., composites for nodular iron) and changing the manufacturing approach, there may be an opportunity to build inexpensive, simple large-diameter structures that are light-weight. Spooner et al. explored lightweight spoked structures to reduce the structural mass of the stator by 70% to 80% [13]. They used an ironless stator for low power machines; however, this spoked design can be implemented for high-power, iron machines, provided new geometries can be created to maintain strength with decreased total mass.

Zavvos and Mueller [9] analyzed structural designs for large transverse flux permanent-magnet generators for offshore wind applications. Using finite-element analysis with gravitational, torsional, and Maxwell loading scenarios, they calculated deformations on the structure and used topology optimization to achieve a design that was at least 6.8% lighter than baseline designs. Likewise, Zavvos et al. [10] used shape optimization on stator design using ANSYS software to determine areas of mass reduction constraint to deflection criteria. They found a 26% reduction in stator mass from shape optimization alone.

Semi-analytic approaches [14, 15] attempt to define the influence of rotor eccentricity on deflections. Eklund and Eriksson [16] take an experimental approach when measuring the magnetic force of an axial flux permanent magnet generator with an air gap of 7 mm. Several light-weight designs have been proposed in recent years, but their manufacturability and upscaling potentials have not been demonstrated.

Additive manufacturing is a method that realizes new lightweight geometries and is being considered for numerous wind turbine components. Wahlström and Gabrielsson [17] discuss the possibilities for gearboxes with internal channels as well as the ability to “reverse engineer” components. The authors also discuss wind-blade mold manufacturing such as that used by Oak Ridge National Laboratory [24].

Additive manufacturing is also a revolutionary approach to optimize direct drive generators for structural design and deflections by changing the geometric design; AM can be used to realize rapid-prototyping of such a design.

Angrish [18] and Almaghariz et al. [19] explore the feasibility of powder-binder printing for creating sand-cast molds that can print large designs with no induced thermal stresses. When defining a complexity parameter, Almaghariz et al. [19] found that sand-cast-mold printing holds advantage to conventional mold and core approaches at 53% to 54% complexity.

### 1.2 Large-Scale Metal Additive Manufacturing for Electric Machines

A variety of methods exist for large-scale metal additive manufacturing. Common practices include direct metal laser sintering and electron beam melting. Direct metal laser sintering is commonly used for small, detailed parts with the highest print size of 800 mm x 400 mm x 500 mm [21]; however, high thermal stresses require post processing heat treatment. Electron beam melting is faster than direct metal laser sintering, but it requires an enclosed, vacuum atmosphere and thick structure to mitigate X-ray radiation. Both processes use powder as the feedstock.

For large-scale additive manufacturing, both processes are disadvantageous because of large initial capital investment, poor repeatability, low throughput and difficult qualification. Drawing from

the conclusions of rotor optimization for AM [20], powder-binder jetting is a promising additive manufacturing process for stator manufacturing because of its ability to combine printing complex geometries with conventional casting thereby increasing throughput while decreasing cost. By printing a mold of the stator design, weight requirements for the printer bed are met and can be implemented with conventional casting. This process eliminates traditional welding, lamination and labor costs. At least two U.S. manufacturers [22, 23] currently have industrial powder-binder jetting printers capable of printing parts of several meters. In powder-binder jetting, a part is created by alternating layers of powder with a binding agent from an inkjet printer head. This powder can be metal used directly or indirectly to create a sand mold. The latter method is selected for this analysis due to its ability to cast 100% dense metal parts and reduce the capital investment of metal powder. The inkjet print head selectively deposits glue in certain areas to build the sand mold, which is cured via ultraviolet light. A roller ensures that each layer of sand is flat; this process is repeated to create a finished part (Figure. 2).

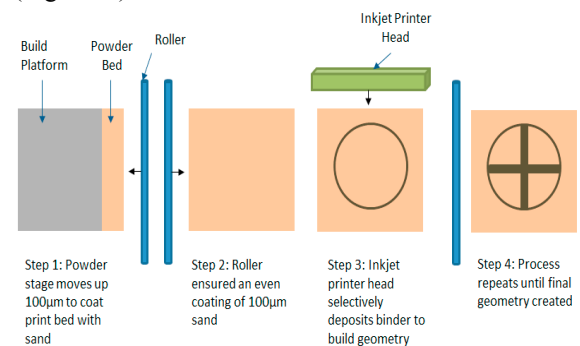


Figure 2: Powder-binder printing schematic

## 2. Approach

A reference structural design was assessed to identify opportunities for weight reduction by optimization of printable complex structural geometries. The conventional spoked-arm design was replaced by alternative design geometries that ensured high strength and low mass. These include:

- (i) a square lattice design with repetitions of support ribbon and spokes distributed radially around the stator, and

- (ii) a U-Beam design with thin lattice structures similar to rotor design considered in a previous study [20].

The designs were parametrized with dimensions for spokes and U-Beams, and structural optimization was performed for each design to remove as much structural material while also ensuring lowest weight and maximum structural stiffness and identifying the best performing designs.

### 2.1. PMDD Reference Design

As the first step, we chose a 5-MW radial flux PMDD machine with an interior rotor arrangement as the reference design. The generator was assumed to be driven by the National Renewable Energy Laboratory (NREL) 5-MW baseline turbine [5], with a rated torque of 4.14 MNm. The drive-line arrangement was similar to the commercial MTorres design described in Stander et al. [4], with the aerodynamic and gravitational loads supported by two main bearings housed on the generator stator-support structure. The stator-support structure consisted of a double-sided, spoked-arm arrangement supporting the yoke teeth and the copper coils. The rotor support structure was a disc or spoked-arm construction supporting the rotor back iron and magnets. The stator-support structure connected the generator to the bedplate allowing transfer of loads. An extensive optimization study was carried out by NREL using GeneratorSE [5] by varying the electromagnetic and structural designs of the spoked-arm and disk-arm combination. Fig. 3 provides a visualization of the stator support structural design and Table 1 lists the design variables.

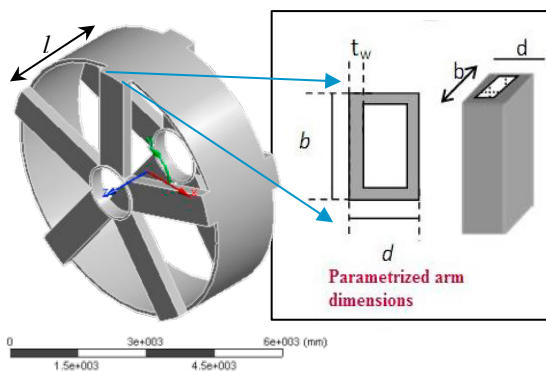


Figure 3: Design variables of a PMDD generator [5]

The structural mass for the baseline 5-MW design with a hollow arm stator design was 18.477 mT [5].

The stator optimization process followed a detailed rotor structural optimization considering AM using a finite-element solver in ANSYS [20]. A design consisting of a plurality of U-Beam spokes was analyzed for structural stiffness, and a 24% reduction in structural mass was achieved after optimization.

Table 1. Tabulated PMDD Design Parameters

Symbol	Design Dimension
$n_s$	Number of stator arms
$h_{ys}$	Thickness of stator back iron
$b_r$	Circumferential arm dimension
$l$	Stator core length
$d$	Arm depth
$t_w$	Arm thickness

### 2.2. Generator Structural Analysis

Since generator loading has the potential to reduce the air-gap between the rotor and stator (typically the air-gap is approximately 1/1000 the diameter), it is important to ensure structural stiffness against the loading conditions. A static structural analysis was performed for the alternative designs using ANSYS considering the loading scenarios and deflection criteria recommended by McDonald [8].

- Gravity: A gravitational force of 9.81 m/s<sup>2</sup> was assumed to act in the negative Z direction and accounts for the worst-case axial deflection possible during transportation.
- Maxwell stress: the normal component of the Maxwell load acting radially due to the magnetic attraction between the rotor magnets and stator coils. The given stress is 0.20 MPa. The Maxwell stress was found using:
 
$$\sigma_{Maxwell} = \frac{\hat{B}_g^2}{2\mu_0} \quad (1)$$
- Centripetal Force: the high torque operation induces a centripetal force that acts along the circumference of the stator in the +Y direction. This was modelled using a shear stress of 40 kPa.

Additional forces due to shear, thermal expansion, forces and moments in the remaining five degrees of freedom exist but were considered negligible in this study. These nontorque loads were assumed to be transferred to the bedplate and do not influence generator structural deflection. Thermal deflections

were also ignored assuming adequate cooling of the generator and its components. The main loading scenarios were considered in finite element analysis to determine the radial, axial and torsional components of stator deflection. These deflections were compared to the maximum allowable deformation limits given by [5]:

- Radial deflection—No more than 10% the air-gap clearance
  - i.  $(0.10)(0.002r_s) = 0.349 \text{ mm}$
- Axial deflection—No more than 2% the axial length
  - ii.  $0.02l_s = 29.78 \text{ mm}$
- Circumferential deflection—No more than  $0.05^\circ$  angle of twist
  - iii.  $\frac{0.05^\circ \pi r_s}{180^\circ} = 3.03 \text{ mm}$

The active mass (mass of materials involved in active flux path) and structural mass (support structures) are computed satisfying the structural deflection constraints and compared to the baseline spoked-arm design. A design of experiments is completed in iterating dimensions of lattice parameters to determine an optimum configuration for the largest stiffness with the lowest mass. Finally, a topology optimization is performed to validate the optimal parameter combination.

### 2.3. Deformation Associated with Changes in Magnetic Loading

Magnet remnant flux density is a variable based on manufacturer, quality and location. The greater this value, the greater the forces experienced by the stator and the greater the deflection. To account for the variability in magnetic loading, the stator deflections associated with remnant flux densities of 1.1 Tesla and 1.4 Tesla were calculated for both designs.

### 2.4. ANSYS Topology Optimization

Topology optimization (TO) is a structural analysis technique that iteratively alters the model geometry to meet user-defined constraint functions (i.e., mass, volume and loading). TO was used as a validation tool to prove that an optimum parameter combination from the design of experiments exists. The final design selected from iterating the design parameters

(lowest mass at lowest deflection) is run through a TO procedure. If no reduction in mass is indicated, then there is initial validation that the design is optimal. In the ANSYS solver, the default compliance scheme was selected. Compliance is defined as the work done on a structure by an applied load. Selecting for a specific mass reduction in the solver corresponded to reducing the volume of the model. As the volume decreased, so did its stiffness, and accordingly, its compliance. The volume was reduced iteratively until a minimum compliance was achieved, or alternatively, until the desired mass/volume reduction was achieved.

## 3. Stator Support Structure Design

The stator design is influenced by the geometry of the supporting structure as well as the nature of bedplate connection. Besides the generator, the nature of bedplate support plays a large role in how much stress must be carried by the stator. As the support and interface increase between the stator and the bedplate, the deflection in the stator decreases. Therefore, several approaches were evaluated for a system-level light-weighting. In the first approach introduced by the authors in [20], the stator structural mass was reduced by creating two stator designs: a square lattice design and a U-Beam spoked lattice design. These structures were lighter, however to compensate for lower structural rigidity, the bedplate connections were altered. As a result, the bedplate carried most of the load resulting in lower deflections. In the second approach, the bedplate is redesigned for reduced mass while keeping the stator geometry constant. A structural and mass analysis was completed for both designs to determine their potential for generator light-weighting.

### 3.1 Square Lattice Design

To make a reasonable comparison and avoid changes to the electromagnetic design, we chose to retain the thickness of the stator cylinder equivalent to that of the baseline stator structural model. A high-strength structure in the form of square lattices was created to fill the space originally occupied by the spoked-arm design. The lattice consisted of unit cells measuring 161.60 mm by 134.97 mm and they were distributed radially around the stator at 50 mm spacing.

Optimization was conducted to remove as much structural material while also ensuring lowest weight.

3.1.1. Design Parameters

The design parameters for the square lattice stator design are shown in Figure 4 and Table 2. For the parametric study, only the height and width of the lattice unit cell were treated as design variables. Within the square lattice design, the bedplate support is along the circumference of the stator. For all stator designs, the support is mirrored about the x-axis to support the stator on both axial ends.

Table 2: Design Parameters of the Square Lattice Geometry

Symbol	Design Dimension
$R$	Stator radius
$h_{ys}$	Stator yoke height
$r_0$	Ring width
$w_l$	Square lattice width
$h_l$	Square lattice height

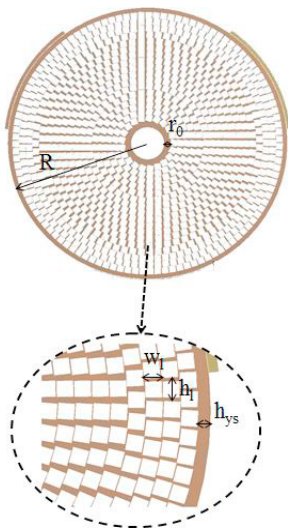


Figure 4: Design parameters for a 5-MW square lattice stator

3.1.2. Mesh Convergence

A mesh convergence study was performed to assess the optimal mesh size for the structural analysis. Figure 5 indicates a 0.85% change with increasing mesh size from 483,000 to 1,559,000 elements. Mesh independence is reached when refinements to the

mesh result in less than 5% change in deflection from previous iterations. Refinement is chosen as a function of the smallest feature size to resolve. As a result, a first order approximation for the parameter optimization can be reached at 952,000 elements to achieve sufficient independence with lower computational expense. Selected mesh parameters included a total mesh sizing of 30 mm.

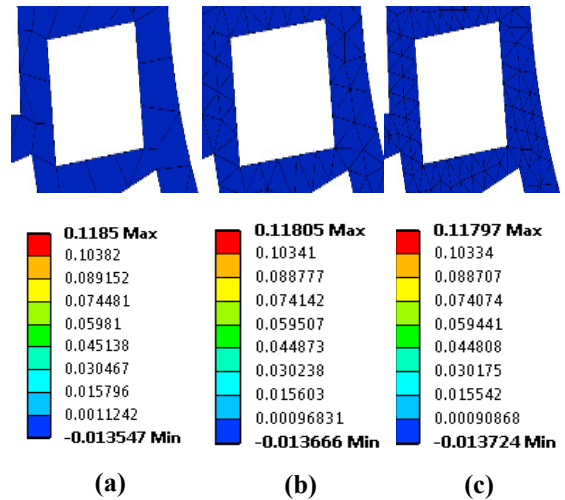


Figure 5: Mesh analysis square lattice showing x-component deflection (in millimetre): (a) 483,000 elements; (b) 952,000 elements; (c) 1,559,000 elements

3.1.3. Parameter Optimization Results

By controlling the unit cell width and height, the parameter optimization of the stator square lattice design was found to significantly decrease the mass of the stator design while maintaining low deflections (Table 3). The radial, torsional and axial deflections were well under defined limits. Deviations between deformations (listed in Table 3 and Figure 5) are due to locations of the bedplate support. Figures 6-8 present results of the directional deflection for the square lattice stator design using ANSYS. The maximum radial deflection was found to be 0.118 mm, the maximum torsional deflection was 0.002 mm, and the axial deflection was 0.319 mm. The critical value for optimization was the radial deflection as greater values run the risk of stator-rotor collision during generator operation.

Table 3: Square lattice parameter optimization results (torque loading)

Symbol	Design Dimension	Optimized Value	Units
$R$	Stator radius	3637	mm
$h_{ys}$	Stator yoke height	87	mm
$r_0$	Ring width	61	mm
$w_l$	Square lattice width	161.60	mm
$h_l$	Square lattice height	134.97	mm
Radial Deformation		0.118	mm
Axial Deformation		0.319	mm
Torsional Deformation		0.002	mm
Structural Mass		13.85	mT
Active Mass		23.29	mT
Total Mass		37.12	mT

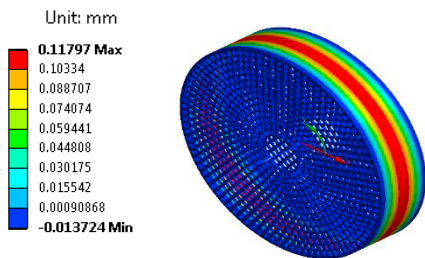


Figure 6: Square lattice radial deflection

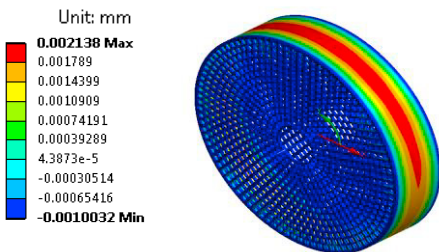


Figure 7: Square lattice torsional deflection

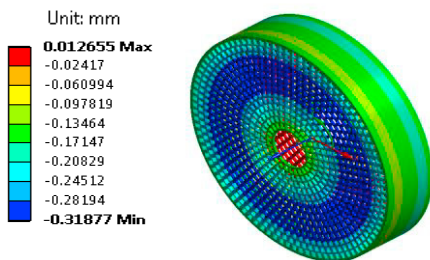


Figure 8: Square lattice axial deflection

### 3.1.4. Deformation Associated with Changes in Magnetic Loading

This study did not attempt to simulate positive feedback conditions or secondary deflections [8] representing stator eccentricity. For flux density changes from 1.1 Tesla to 1.4 Tesla, the worst-case scenario for Maxwell loading increases from 0.643 MPa to 1.04 MPa. Table 4 shows the deflections associated with this scenario.

We used a constant value of 0.20 MPa to depict average generator magnetic loading, which is consistent with NREL’s GeneratorSE [5].

Table 4: Deformation of square lattice design when changing remnant flux densities

Component Deformations	Units	$B_r=1.1$ Tesla	$B_r=1.4$ Tesla
Radial deformation	mm	0.186	0.291
Torsional deformation	mm	0.178	0.286
Axial deformation	mm	0.032	0.053

### 3.1.5. Topology Optimization of Square Lattice Design

Following the parameter optimization, a topology optimization was performed to determine areas of further mass reduction (Figure 9). Areas of further mass reduction suggested by topology optimization for the square lattice stator design include:

- Reduce the width of the inner disk
- Introduce voids within the lattice dimensions.

Note that the topology optimization results indicate less areas for mass reduction potential indicating the design is considered optimized. Option b in Figure 9 is rejected, as introducing small voids increases the risk of crack propagation in the stator.

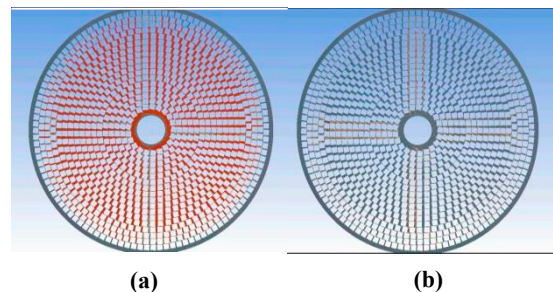


Figure 9: Topology optimization results for 5-MW square lattice stator design (a) pre-topology optimization (red indicates locations of void introductions) (b) post-topology optimization (yellow indicates locations of thinner supports).



### 3.2 U-Beam Spoked-Lattice Design

Drawing from the success of the U-Beam spoked web design of the rotor [20], the stator incorporates this design with thinner lattice structures and is mirrored about the x-axis.

#### 3.2.1 Design Parameters

Parameters for the U-Beam spoked-lattice stator design are shown in Table 5. Differences between the rotor design [20] and stator designs include decreased lattice thickness and width as well as increased arm count with decreased arm width. Lower widths and thicknesses can be achieved as the stator supports are mirrored across the x-axis. Therefore, to match the structural mass seen on the rotor, each U-Beam spoked-lattice assembly (Figure 10) must be half the mass of that on the rotor.

Table 5: 5-MW U-Beam spoked-lattice stator design variables

Symbol	Design Dimension
$w_d$	Disk width
$w_r$	Ribbon width
$t_r$	Ribbon thickness
$w_u$	U half width
$w_s$	U spoke width
$h_u$	U height
$h_b$	U base height
$n_{spokes}$	Number of spokes

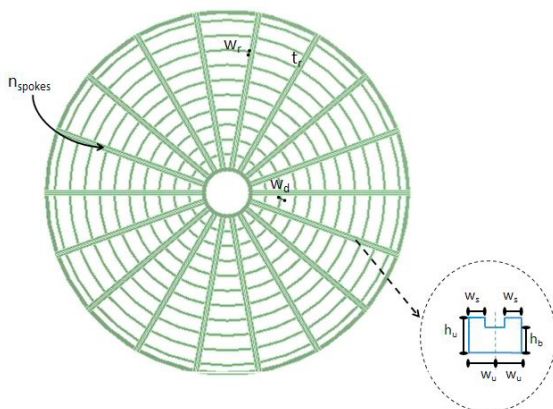


Figure 10: Design parameters for a 5-MW U-Beam spoked-lattice stator

#### 3.2.2 Mesh Convergence

Figure 11 suggests that the results change by less than 5% when increasing mesh size from 503,303 to 1,940,066 elements. Hence it was decided to choose the mesh with 503,303 elements. To ensure a high degree of accuracy, further refinement was made with a lattice mesh size of 20 mm resulting in a mesh with 1,272,085 elements.

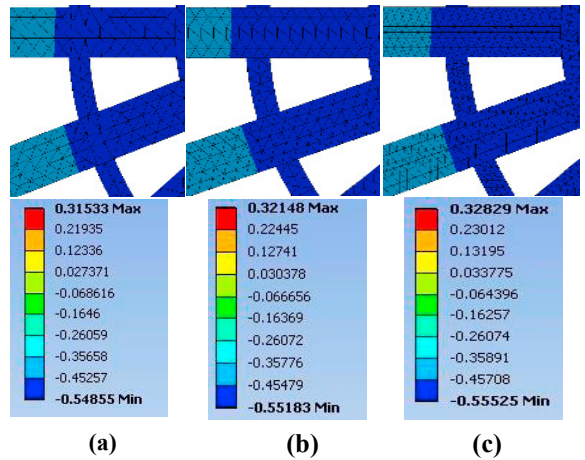


Figure 11: Mesh independence analysis showing x-component deflection (in millimetre) of U-Beam spoked-lattice design: (a) 503,303 elements (b) 1,038,366 elements (c) 1,940,066 elements

#### 3.2.3 Parameter optimization results

Parameter optimization of the U-beam spoked-lattice stator design was found to decrease the mass of the stator design with low deflections (Table 6).

Table 6: 5-MW stator U-Beam spoked-lattice optimization results (torque loading)

Symbol	Design Dimension	Optimized Value	Units
$w_d$	Disk width	86.13	mm
$w_r$	Ribbon width	54.91	mm
$t_r$	Ribbon thickness	38.60	mm
$w_u$	U half width	61.97	mm
$w_s$	U spoke width	42.68	mm
$h_u$	U height	45.00	mm
$h_b$	U base height	38.60	mm
$n_{spokes}$	Number of spokes	17	-
	Radial deformation	0.534	mm
	Axial deformation	1.609	mm
	Torsional deformation	0.448	mm
	Structural mass	8.70	mT
	Active mass	23.24	mT
	Stator mass	31.94	mT

Figures 12-14 show the results of directional deflection for the U-Beam spoked-lattice stator design using ANSYS. Note that the maximum radial, torsional and axial deflections were 0.53 mm, 0.45 mm and 1.61 mm, respectively. Although torsional deflection is greater than the allowable value, this can be minimized by re-evaluating the bedplate design. This consideration allows the lightweight U-Beam spoked-web model to be considered for optimal lightweight stator development.

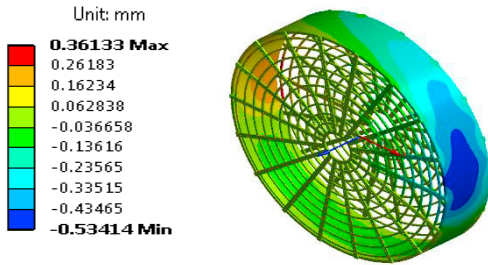


Figure 12: Radial deflection of U-Beam spoked-lattice stator

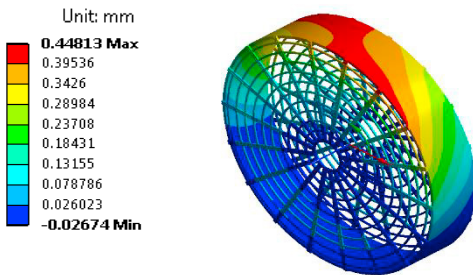


Figure 13: Torsional deflection of U-Beam spoked-lattice stator

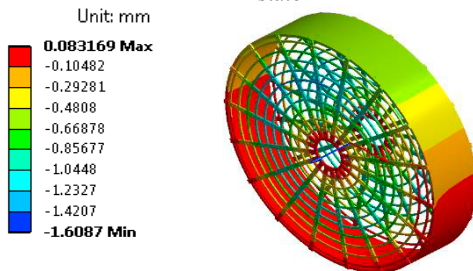


Figure 14: Axial deflection of U-Beam spoked-lattice stator

3.2.4 Deformation varying magnetic loading

Table 7 depicts deformation associated with the stator U-Beam spoked-lattice design under the two extreme cases of magnetic loading. It is apparent that greater flux density corresponds to greater stator deflections.

Table 7: Stator deflections associated with different magnet remnant flux densities

Deformation components	Units	$B_r=1.1$ Tesla	$B_r=1.4$ Tesla
Radial Deformation	mm	3.28	5.08
Torsional Deformation	mm	3.08	4.70
Axial Deformation	mm	3.11	4.30

4. Influence of Bedplate Support

In the conventional spoked-arm stator design, the stator structure is connected to the bedplate at its inner ring, which holds the bearings. Loads from the turbine rotor are transferred from the main shaft and bearings to the tower through this bedplate connection; however, the location of the bedplate supports strongly influences deflections within the stator. A trade-off exists between a heavier stator carrying a greater share of the loads and a lighter stator with heavier bedplate carrying the bulk of the loads.

4.1 Altering the Bedplate Support Location

An optimized connection to the bedplate or support location can greatly minimize the stator deformation (Figure 15). To evaluate the potential, bedplate supports were located on the bottom 40% of the lattice circumference and connected by a shaft through a center hole on one side and supported at the other side on the opposite plane.

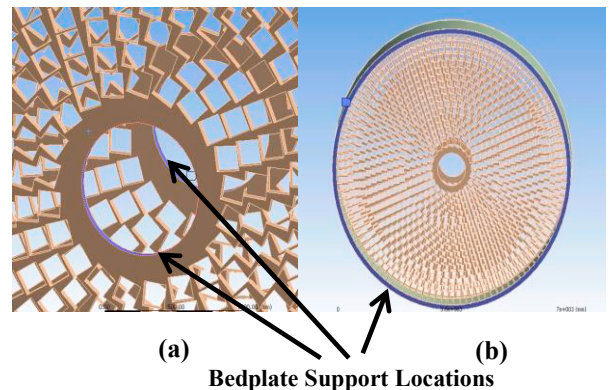


Figure 15: Stator bedplate support locations: (a) conventional support (b) altered bedplate connection

As may be inferred from Table 8, the altered bedplate design can significantly reduce the deformation of the optimized square lattice design with conventional bedplate support. Note there is a significant increase in deformation associated with supporting the stator by the thickness of the inner ring. As such, a lightweight stator design can be obtained with reduced deformations by altering the bedplate design.

Table 8: Deformation of square lattice structures under different bedplate support cases

Deformation Components	Units	Conventional Bedplate Support	Altered Support
Radial deformation	mm	7.67	0.155
Torsional deformation	mm	87.7	0.096
Axial deformation	mm	1.43e-4	9.11e-3

## 5. Generator Light-Weighting Potential with AM

Combined with rotor structural mass reductions, an optimized stator holds potential for further total generator mass reduction. The stator has greater design variability than the rotor as loading can be transferred to new bedplate designs to reduce the structural mass of the stator. For a radial flux PMDD with the stator outside of the rotor, a larger outer stator diameter results in higher active stator mass. Therefore, should the stator alone support all loading conditions, its structural mass must greatly increase. To reduce structural mass and allow stator optimization, it is assumed that the bed plate design supports the stator along part of or the entire circumference of the stator. As a result, the stator structural mass can be optimized.

Both the square lattice and U-Beam spoked-lattice stator designs provide for structural mass savings. Total generator structural mass reductions are given on a per generator basis assuming the rotor structural mass is 12.4 mT observed in a previous rotor optimization study [20]. When compared to NREL's GeneratorSE baseline design [5], the total rotor and stator structural mass reduction using AM designs is achieved. For the optimized square lattice stator design, a 25% mass reduction is seen, an 8.80 mT mass reduction. For the optimized U-Beam spoked-lattice design, a 39% mass reduction is achieved, equivalent to a 13.728 mT mass reduction. Therefore,

using an AM optimized rotor and stator has the potential for generator weight savings up to 39%.

## 6. Conclusions

Additive manufacturing allows designers to exploit a greater number of constraints than traditional manufacturing techniques. Designing for light weight and strength often includes periodic repetitions of eccentric geometries. Furthermore, geometries such as the U-Beam spoked-lattice and square lattice designs are reasonably manufactured only through additive techniques. The results of this stator optimization study provide the following key insights:

- Powder-binder jetting of a sand-cast mold holds the potential for manufacturing complex stator geometries.
- The lightest stator structural design is the U-Beam spoked-lattice.
- Incorporating the U-Beam spoked lattice stator design with the U-Beam spoked lattice rotor design can result in up to 39% generator structural mass savings.
- Stator bedplate support greatly influences stator deflection. In the conventional bedplate case, deflections for the lightweight designs are above critical limits. However, by altering the bedplate design to support the stator around the circumference, deflections can greatly decrease as the bedplate is made to carry bulk of the load.

## 7. Future Work

We plan to combine stator design modeling with bedplate design optimizing for total mass and stator structural rigidity. Further work is planned to:

- Develop accurate rotor and stator costing model for AM.
- Optimize the rotor, stator and bedplate together for system-level modeling for greatest mass reduction
- Create a scaled version of the designs and perform deflection testing for validating the results.

## 8. Acknowledgements

This work was supported in part by the U.S. Department of Energy under Contract No. DE-AC36-08GO28308 with the National Renewable Energy Laboratory, and the Office of Science, Office of Workforce Development for Teachers and Scientists under the Science Undergraduate Laboratory Internships Program. Funding for the work was provided by the DOE Office of Energy Efficiency and Renewable Energy Wind Energy Technologies Office.

The authors acknowledge results of detailed study by McDonald (2008) that sheds insight into the elastic behavior of spoked arm designs.

The U.S. government retains and the publisher, by accepting the article for publication, acknowledges that the U.S. government retains a nonexclusive, paid-up, irrevocable, worldwide license to publish or reproduce the published form of this work, or allow others to do so, for U.S. government purposes.

## References

- [1] A. Tassarolo, F. Luise, S. Pieri, A. Benedetti, M. Bortolozzi and M. De Martin., Design for Manufacturability of an Offshore Direct-Drive Wind Generator: An Insight Into Additional Loss Prediction and Mitigation, *IEEE Transactions On Industry Applications*, VOL. 53, NO. 5, September/October 2017.
- [2] P. Dvorak, Axial flux generator ready to take weight and problems out of nacelles, <https://www.magnax.com/magnax-blog/axial-flux-generator-ready-to-take-weight-and-problems-out-of-nacelles>, 22 October 2017, [Accessed: March 2018].
- [3] GE's Haliade\*150-6MW High yield offshore wind turbine, [https://www.gerenewableenergy.com/content/dam/gepowerrenewables/global/en\\_US/downloads/brochures/wind-offshore-haliade-wind-turbine.pdf](https://www.gerenewableenergy.com/content/dam/gepowerrenewables/global/en_US/downloads/brochures/wind-offshore-haliade-wind-turbine.pdf), [Accessed: March 2018].
- [4] J. N. Stander, G. Venter, M. J. Kamper, "Review of direct-drive radial flux wind turbine generator mechanical design," *Wind Energy* 15 (2011): 459–472, doi:10.1002/we.484
- [5] L. Sethuraman and K. Dykes., "Generator SE, A Sizing Tool for Variable Speed Wind Turbine Generators," Technical Report NREL/CP-5000-66462, National Renewable Energy Laboratory, Golden, Colorado, September 2017.
- [6] H. Li, Z. Chen, and H. Polinder. 2006. Research report on models for numerical evaluation of variable speed different wind generator systems. UpWind deliverable No: D 1B2. b.2.
- [7] D. Bang. "Design of Transverse Flux Permanent Magnet Machines for Large Direct Drive Wind Turbines", PhD Thesis, TU Delft, The Netherlands, 2010.
- [8] A. S. McDonald, M. A. Mueller. 2008. Development of Analytical Tools for Estimating Inactive Mass, University of Edinburgh, Scotland, UpWind report, 2008.
- [9] A. Zavvos, "Structural optimization of permanent magnet direct drive generators for 5MW wind turbines," PhD Thesis, University of Edinburgh, 2013.
- [10] A. Zavvos, A. McDonald, and M. Mueller, "Structural optimisation tools for iron cored permanent magnet generators for large direct drive wind turbines," IET Conference on Renewable Power Generation (RPG 2011), 2011.
- [11] R.S. Semken, Lightweight, Liquid-Cooled, Direct-Drive Generator For High-Power Wind Turbines: Motivation, Concept, And Performance, PhD Thesis, Lappeenranta University of Technology, Lappeenranta, Finland, 2015.
- [12] M. Garibaldi, C. Gerada, I. Ashcroft, R.Hague, H. Morvan. The Impact of Additive Manufacturing on the Development of Electrical Machines for MEA Applications: A Feasibility Study. MEA2015, More Electric Aircraft, Feb 2015, Toulouse, France.
- [13] E. Spooner, "Lightweight, ironless-stator, PM generators for direct-drive wind turbines," Second IEE International Conference on Power Electronics, Machines and Drives, vol. 152, Jan. 2004.
- [14] Z, Q. Zhu, L.J. Wu and M.L. Jamil, "Influence of pole and plot number combinations on cogging torque in permanent magnet machines with static and rotating Eccentricities." *IEEE Trans. Industry Applications*, pp. 1-13, 2014.
- [15] D. Palani, Z. Azar, A. Thomas, Z. Q. Zhu, and D. Gladwin, "Modeling technique for large permanent magnet generators accounting for manufacturing tolerances and limitations," 2016 XXII International Conference on Electrical Machines (ICEM), Lausanne, 2016.
- [16] P. Eklund and S. Eriksson, "Air gap magnetic flux density variations due to manufacturing tolerances in a permanent magnet synchronous generator", XXII International Conference on Electrical Machines (ICEM), Lausanne, 2016.

- [17] N. Wahlström, “Additive Manufacturing Applications for Wind Turbines,” MSc Thesis, KTH Industrial Engineering and Management, Stockholm, Sweden, 2017.
- [18] A. Angrish, “A critical analysis of additive manufacturing technologies for aerospace applications,” IEEE Aerospace Conference, Big Sky, MT, 2014.
- [19] E. S. Almaghariz, “Determining when to use 3D sand printing: quantifying the role of complexity,” M.S Thesis, Youngstown State University, 2015.
- [20] A. Hayes, L. Sethuraman, and L. J. Fingersh, “Structural Mass Saving Potential of a 5MW Direct Drive Generator Designed for Additive Manufacturing,” in International Conference on Future Technologies for Wind Energy, Boulder, Colorado, 2017.
- [21] Concept Laser, “DMLS Machines,” Metal 3D printers -Concept Laser. Available: <https://www.concept-laser.de/en/products/machines.html>. [Accessed: February 2018].
- [22] “Inside ExOne,” English. Available: <http://www.exone.com/>. [Accessed July 2017].
- [23] voxeljet.com, “Industrial 3D printer | voxeljet solutions,” voxeljet.com. Available: <https://www.voxeljet.com/>. [Accessed: July 2017].
- [24] Oak Ridge National Laboratory. (2016). Transforming Wind Turbine Blade Mold Manufacturing with 3D Printing (United States, Department of Energy, EERE). Washington, D.C. Available: <https://www.energy.gov/sites/prod/files/2016/08/f33/3D-printed-blade-mold-fact-sheet-08032016.pdf>. [Accessed March 2018].